Desalination and Water Treatment
www.deswater.com

21 (2010) 346–356
September

1944-3994/1944-3986
doi: 10.5004/dwt.2010.1441

Modeling and simulation of a new design of the SMCEC desalination unit using solar energy

Khalifa Zhani[a], Habib Ben Bacha[b]*

[a]*Laboratoire des Systèmes Electro-Mécaniques (LASEM), National Engineering School of Sfax - Sfax University, Tunisia*
[b]*College of Engineering in Alkharj, King Saud University, BP 655-11946, Kingdom of Saudi Arabia*
Tel. +966506678408, Fax. +9661553964; email: hbacha@Ksu.edu.sa

Received 8 November 2009; accepted 8 March 2010

ABSTRACT

This paper deals with modeling and simulation of a new design of the SMCEC (Solar Multiple Condensation Evaporation Cycle) desalination unit using solar energy. The newly designed system is basically composed of a flat plate solar air collector, a flat plate solar water collector, a humidifier, an evaporation tower and a condensation tower. A mathematical model based on heat and mass transfers in each component of the unit is developed and simulated using C++ software in a steady state regime. The numerical model is used to investigate the steady state behavior of each component of the unit exposed to a variation of the entrance parameters and meteorological conditions. This theoretical model is expected to help in predicting the behavior of the unit in various operating and climatic conditions. Besides, it would be useful in enhancing the performance of such unit.

Keywords: Solar energy; Water desalination; Steady state; Modeling; Simulation

1. Introduction

Fresh water scarcity, fossil energy depletion and environmental degradation due to gas emissions pose increasing challenges in many countries, particularly in the urban area of arid and semiarid regions. The immediate response to counter these challenges is coupling desalination processes with renewable energy resources such as solar energy and geothermal water. In Tunisia, as throughout the world, a growing number of municipalities are implementing a development program focusing on the use of renewable energies for brackish and seawater desalination to provide fresh water for some remote regions.

Conventional desalination process, such as multi-stage flash (MSF), multi-effect (ME), vapor compression (VC) and reverse osmosis (RO) are designed to provide water for much larger communities and are usually constructed over a long period of time. These require a great amount of energy to operate, infrastructure to be constructed and a significant amount of piping and pumps to transport the fresh water. Many countries in the Middle East, because of oil income, have enough money to invest in and run desalination equipment. The installed capacity of desalinated water systems in year 2000 is about 22 million m^3/day and is expected to increase drastically in the next decades. It has been estimated that the production of 22 million m^3/day requires about 203 million tons of oil per year. Given current understanding of the greenhouse effect and the importance of CO_2 levels, this use of oil is debatable [1].

Small scale standalone solar powered desalination systems are becoming more popular throughout the world and only a handful of similar systems have been

*Corresponding author

produced. These small scale standalone desalination systems are much more versatile being able to be used in a variety of environments, relatively simple to design, less time to implement and having smaller production cost. Creating a low cost sustainable desalination system would provide small, remote communities with the fresh water required to drink and to irrigate small areas of land allowing a range of crops to be farmed which could benefit the economy.

According to literature review, there are many investigators who have developed and studied various standalone solar desalination systems using the humidification/dehumidification principle. The following is a summary of some of the literature studies.

In 1999, a solar desalination unit based on the SMCEC principle (Solar Multiple Condensation Evaporation Cycle) was built by Ben Bacha et al. [2] in Tunisia. The SMCEC based desalination unit consists of three main parts: 7.2 m^2 of flat plate water solar collector, condensation tower and evaporation tower. Thorn trees were used for evaporator and condenser was constructed from polypropylene plates. The thermal insulation of chambers was achieved by the plates of polypropylene which covered the whole internal surface of chambers and protected the external insulating styrofoam layer against corrosion. Presented curves show that production of the unit at humidifier inlet water temperature of 70°C, is 7.2 kg/h. Based on model simulation and experimental validation, the optimum operation and production for this type of system need a perfect insulation of the unit, a high water temperature and flow rate at the entrance of the condenser, hot water recycling by injection at the top of the evaporation chamber and a storage tank to store the hot water excess that would extend water desalination beyond sunset.

In 2009, Soufari et al. [3] constructed a pilot unit with a capacity of 10 kg/h which was located at Iranian Research and Development Center for Chemical Industries (IRDCI), Karaj, Iran. This unit includes 28 m^2 of flat plate water solar collector, a humidifier and a dehumidifier. The design of this unit is similar as the SMCEC one but different in type of construction materials and dimensions.

In 2004, Ben Amara et al. [4] designed and constructed a pilot solar desalination unit based on Multi-Effect Humidification/ Dehumidification (MEH) in Tunisia. The main parts of the fabricated unit consist of a heat equipment device (heat exchanger), a spray humidifier and a dehumidifier system. This equipment was used to simulate the seawater desalination process experimentally with an eight-stage air solar collector heating-humidifying system. In another work, Ben Amara et al. [5] highlighted the major shortcoming of this solar desalination unit. In fact, the only use of air solar collector as thermal energy supplier to such solar desalination unit is a deficiency in case of low solar radiation because air solar collectors are very sensitive to solar radiation fluctuation. Indeed, with the rapid response of the collector to solar fluctuations, the air collector temperature drops quickly, resulting in condensation in the chamber and a decrease in performance of the whole solar desalination process. This shortcoming was experimentally verified.

In the same year, Orfi et al. [6] presented a theoretical study of a SDHD (Solar Desalination with Humidification Dehumidification) process at Monastir, Tunisia. The SDHD unit includes air and water solar collectors and a separate evaporator and condenser. In order to improve the heat and mass exchange, five parallel plates made of wood and covered with textile (cotton) were fixed in the evaporator. Both the condensation and evaporation chambers were horizontal and had a rectangular cross section. They have conducted various simulations, showing the effects of the relevant non dimensional parameters on the daily and yearly fresh water production. Maximum reported value for production of this unit was 1.3 L/h.

Many other investigators [7–11] have developed and constructed different humidification–dehumidification desalination process in two separate columns, one for humidification and another for dehumidification, with the columns constructed in different geometries with various materials. However, separate geometry increases the complexity of the system, the capital cost and heat losses. In addition, in case of using a separate humidification column, the latent heat of evaporation for humidification can only come from the sensitive heat of saline water fed to humidify the carrier gas, which limits the amount of the water that can be vaporized, resulting in a limited humidification effect of the carrier gas. This, in its turn, limits the fresh water production of such a unit.

It is clear from the previously cited works that the major drawback of standalone solar desalination unit based on humidification/dehumidification principle is their limited fresh water production which in some cases isn't able to compete solar distiller fresh water production. So, to overcome the shortcomings of developed solar desalination unit which are mentioned previously in literature review and to ameliorate the fresh water production of such unit especially the SMCEC unit, we have integrated into the latter a flat plate air solar collector for heating air and a humidifier for subsequent humidification. Then, the newly designed system is essentially composed of a flat plate solar air collector, a flat plate solar water collector, a humidifier and a distillation module which is composed of an

evaporation tower and condensation tower. The integration of both air solar collector and a humidifier into the SMCEC unit is based upon the fact that the vapour carrying capability of air increases with temperature: 1 kg of dry air can carry 0.5 kg of vapour and about 670 kcal when its temperature increases from 30 to 80°C [12].

The current solar desalination system studied in this paper differs from earlier published works presented previously by the following points:

- It requires a low level of maintenance from unskilled operators by using dismantled equipments.
- The simultaneous heating of air and water respectively by air solar collector and water solar one in order to increase the thermal performance of the system.
- The simultaneous utilization of evaporation chamber and a humidifier to increase the quantity of evaporated water. Therefore, to improve the fresh water production.
- The integration of the evaporation chamber and the condensation chamber in one module called distillation module in order to increase the thermal and mass transfers of the produced steam quantity toward the condensation chamber to improve the rate of condensed water.
- The optimization of the energy recuperation of the heating system.

In two previous papers [13,14], we present the detail development of the mathematical models and the effect of different operating modes on fresh water production. The paper at hand deals with mathematical modeling and numerical simulation of each unit component of the developed unit.

The present paper is organized as follows. Sections 2 and 3 are dedicated, respectively, to the process description and the formulated mathematical models. The simulation results are discussed in Section 4.

2. Process description

Fig. 1 shows a schematic diagram for the humidification-dehumidification process. The main components of the unit are the air and water solar collectors, the humidifier and the distillation module. The water solar collector use a sheet-and-tube, in copper material, absorber with the tubes as an integral part of the sheet. The air solar collector is a flat plate one and is formed by a single glass cover and an absorber. The humidifier, also called cooling tower, is used in many chemical processes. In the desalination process, the humidifier is used to separate clean water from the salt water. This is essentially an extraction process. The humidifier used in the desalination unit is a pad one. The distillation module consists of air humidifier (evaporator) and dehumidifier (condenser). The condenser is constituted of vertical tubes disposed in alternate rows as shown in Fig. 2.

The principle of functioning of this desalination process is as follows:

Sea or brackish water which is preheated in the condensation tower, by the latent heat of condensation, and heated in the water solar collectors is pulverized into the humidifier and the evaporation tower. Due to heat and mass transfers between the hot water and the heated air stream in the humidifier in case of working in open air loop and between the hot water and the dehumidified air stream, coming from the condensation tower, in the evaporation tower in case of working in closed air loop, the latter is loaded by moisture. To increase the surface of contact between air and water, and therefore to rise the rate of air humidification, packed bed is implanted in the tower of evaporation and the humidifier. The saturated moist air is then transported toward the tower of condensation where it comes in contact with a surface the temperature of which is lower than the dew point of the moist air. The condensed water was collected from the bottom of the condensation tower, while the brine (the salty water exiting the evaporator and the humidifier) at the bottom of both the humidifier and evaporation tower will be either recycled and combined with the feed solution at the entry point or rejected in case of increase of saltiness rates.

3. Process modeling

The first stage of all survey of a physical process requires its representation by a mathematical model. We have developed a mathematical model in steady state regime based on heat and mass transfers in each component of the unit viz. water solar collector, air solar collector, humidifier and distillation module (evaporation tower and condensation tower) of the desalination unit in order to numerically simulate the HD system. The resulting system of equations was solved using the Orthogonal Collocation method. The developed models allow a good description of the real process and a better monitoring of the spatial distribution of the different parameters like air and water temperatures and air humidity.

- The water solar collector mathematical model

The energy balance equation for the system formed by the absorber and the fluid for a slice of the collector with a width of l, a length of dx and a surface of ds, is the next one:

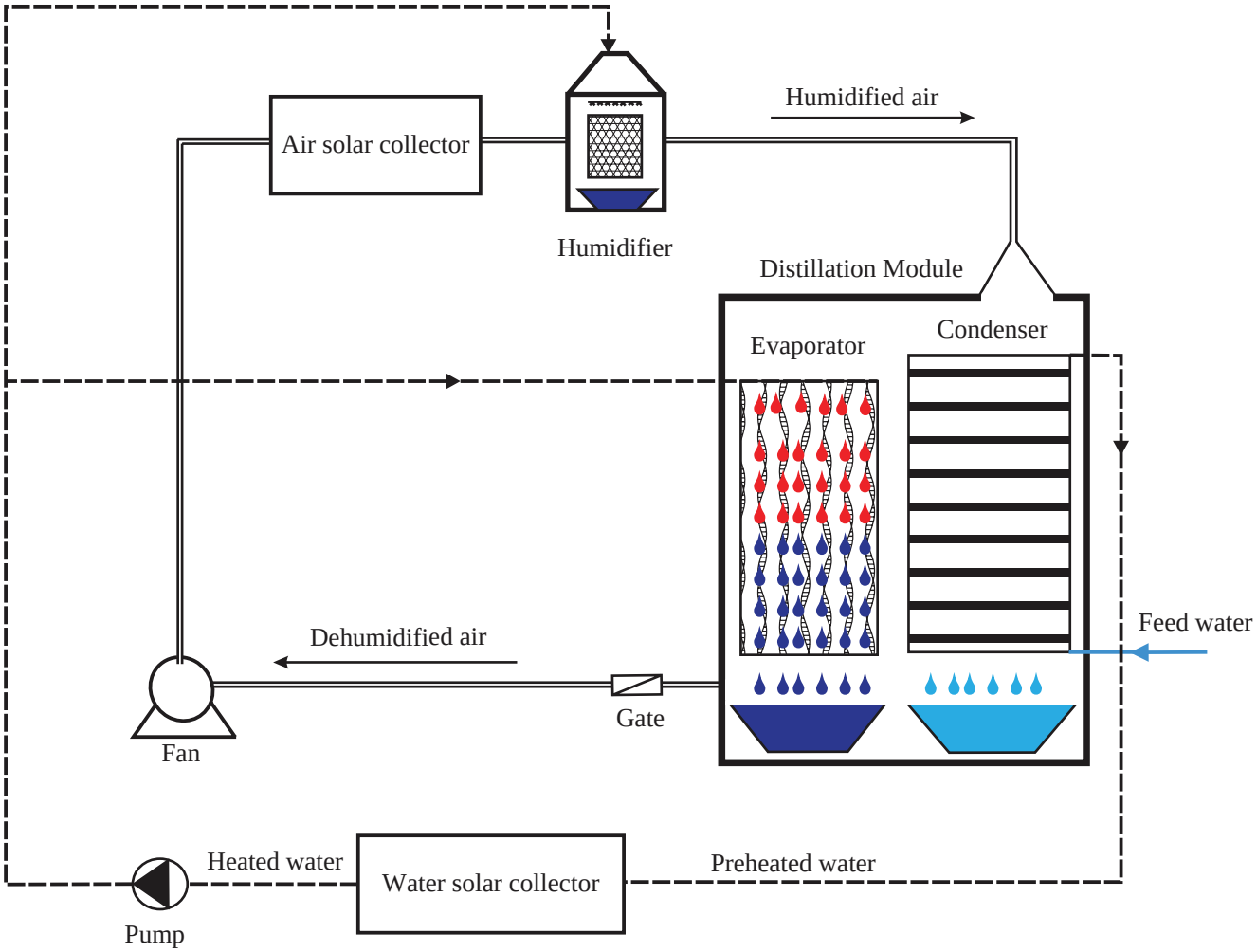

Fig. 1. Schematic diagram of the solar desalination system.

$$\frac{dT_w}{dx} = \frac{U_w l}{m_w C_w}\left(\frac{BI}{U_w} + T_{amb} - T_w\right). \quad (1)$$

• The air solar collector mathematical model

The thermal balances of the system formed by the absorber, air and the glass cover for a slice of the collector surface are the followings:

At the absorber plate

$$I\tau_v\alpha_{pl} = h_{radpl-v}(T_{pl} - T_v) + U_{loss}(T_{pl} - T_{amb}) + h_{conpl-a}(T_{pl} - T_a). \quad (2)$$

At the flowing air

$$\frac{dT_a}{dx} = \beta_1(T_{pl} - T_a) + \beta_2(T_v - T_a), \quad (3)$$

with $\beta_1 = \frac{bh_{conpl-a}}{m_a C_a}$ and $\beta_2 = \frac{bh_{conv-a}}{m_a C_a}$

At the glass covers

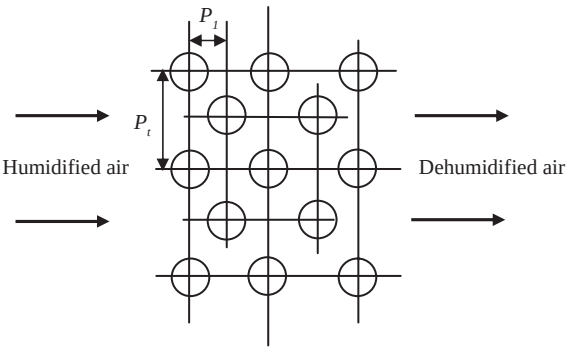

Fig. 2. Staggered tubes layout.

$$I\alpha_v = h_{radv-pl}\,(T_v - T_{pl}) + h_{conv-a}(T_v - T_a) + h_{v-amb}(T_v - T_{amb}), \quad (4)$$

with: $h_{v-amb} = h_{conv-amb} + h_{radv-amb}$; overall heat transfer coefficient toward outside

• The humidifier mathematical model
– Heat and masse balances

At the air phase

$$\frac{dT_g}{dx} = \frac{h_g a_h (T_g - T_i)}{m_g C_g}. \quad (5)$$

At the water phase

$$\frac{dT_L}{dx} = \frac{h_L a_h (T_i - T_L)}{m_L C_L}. \quad (6)$$

At the air–water interface

$$\frac{dW_g}{dx} = \frac{K_m a_h (W_i - W_g)}{m_g}. \quad (7)$$

– Enthalpy balances

$$m_L C_L dT_L = m_g C_g dT_g + m_g \lambda_o dW_g. \quad (8)$$

The curve of saturation of water steam is given by the following equation [15]:

$$W_i = 0.62198 \frac{P_i}{1 - P_i}. \quad (9)$$

• The evaporation tower mathematical model

At the air phase

$$\frac{dT_{g,ev}}{dz} = \frac{h_g a_{ev} (T_{i,ev} - T_{g,ev})}{m_{g,ev} C_{g,ev}}. \quad (10)$$

At the water phase

$$\frac{dT_{L,ev}}{dz} = \frac{h_L a_{ev} (T_{L,ev} - T_{i,ev})}{m_{L,ev} C_L}. \quad (11)$$

At the interface air–water

The mass balance equation at the interface level is given by the following one:

$$\frac{dW_{g,ev}}{dz} = \frac{K_m a_{ev} (W_{i,ev} - W_{g,ev})}{m_{g,ev}}. \quad (12)$$

The thermal balance equation can be written under the following form:

$$h_L a_{ev} (T_{L,ev} - T_{i,ev}) = h_g a_{ev} (T_{i,ev} - T_{g,ev}) + \lambda_o K_m a_{ev} (W_{i,ev} - W_{g,ev}). \quad (13)$$

The curve of saturation of water steam is given by the following equation:

$$W_{i,ev} = 0.62198 \frac{P_{i,ev}}{1 - P_{i,ev}}. \quad (14)$$

• The condensation tower mathematical model
– Heat and mass balances

At the water phase

$$\frac{dT_e}{dz} = \frac{UA(T_{ic} - T_e)}{D_e C_e}. \quad (15)$$

At the air phase

$$\frac{dT_{gc}}{dz} = \frac{h_{gc} A (T_{gc} - T_{ic})}{m_{gt} C_{gc}} + \frac{\lambda_o K_{mc} A (W_{gc} - W_{ic})}{m_{gt} C_{gc}}. \quad (16)$$

At the interface air-condensate

The mass balance equation at the interface air-condensate level is given by the following equation:

$$\frac{dW_{gc}}{dz} = \frac{K_{mc} A (W_{ic} - W_{gc})}{m_{gt}}. \quad (17)$$

The thermal balance equation at the interface air-condensate can be written as follows:

$$W_{ic} = W_{gc} + \frac{h_{gc} (T_{gc} - T_{ic}) + U(T_e - T_{ic})}{\lambda_o K_{mc}}. \quad (18)$$

The water condensation rate is determined by using an algebraic equation that relates the variation of the water content with the height of the tower:

$$dm_c = K_{mc} A (W_{ic} - W_{gc}) dz. \quad (19)$$

The saturation absolute humidity is given by the following equation:

$$W_{ic} = 0.62198 \frac{P_{ic}}{1 - P_{ic}}. \quad (20)$$

– Heat transfer correlations

Table 1
Air film heat transfer correlations (h_{gc}) [18]

Regime	Range	heat transfer coefficient
Laminar	$1 < Re < 50$	$h_{gc} = \frac{\lambda_{gc}}{d_e}\ 1.04\ Re^{0.4}\ Pr^{0.36}$
	$50 < Re < 10^3$	$h_{gc} = \frac{\lambda_{gc}}{d_e}\ 0.71\ Re^{0.5}\ Pr^{0.36}$
Transient	$10^3 < Re < 2 \times 10^5$	$h_{gc} = \frac{\lambda_{gc}}{d_e}\ 0.35\left(\frac{P_t}{P_l}\right)^{0.2}\ Re^{0.6}\ Pr^{0.36}$
Turbulent	$Re > 2 \times 10^5$	$h_{gc} = \frac{\lambda_{gc}}{d_e}\ 0.031\left(\frac{P_t}{P_l}\right)^{0.2}\ Re^{0.8}\ Pr^{0.4}$

The overall heat transfer coefficient, from the air-condensate interface to the cooling water inside the condenser, based on outer surface area of the tubes is evaluated using [16,17]:

$$\frac{1}{U} = \frac{1}{h_e\left(\frac{d_e}{d_i}\right)} + \frac{1}{h_c} + R_{ee}\left(\frac{d_e}{d_i}\right) + R_{ec} + \frac{d_e}{2\lambda_p} Log\left(\frac{d_e}{d_i}\right).$$

The effect of fouling on heat transfer coefficient was considered in this model. The fouling resistance was used on inner and outer tube surfaces R_{ee} and R_{ec}, respectively.

The air film heat transfer coefficient for cross flow to a staggered tube bundles is presented in Table 1 for laminar, for transition and for turbulent flow.

The heat transfer correlation between water and inside vertical tube surface of the condensation tower is presented in Table 2 for laminar, for transition and for turbulent flow.

The mean heat transfer coefficient for the condensate film is expressed using Nusselt relation [20]

$$h_c = 0.943\left(\frac{g\rho_c^2\lambda_c^3\lambda_o}{L\mu_c(T_{ic} - T_p)}\right)^{\frac{1}{4}}.$$

4. Simulation results and discussion

The below simulation results were obtained for the properties of the entire desalination unit which are shown in Table 3.

Figs. 3 and 4 show the influence of inlet fluid temperatures on the outlet ones respectively for the water and air solar collectors.

From Fig. 3, one can deduce that for the low values of T_{wi}, T_{wo} can have high ones. For example, for a value of T_{wi} equal to 15°C, T_{wo} takes a value of the order of 42°C, that is to say one can have a gain of heating equal to 64.28%, while for a value of T_{wi} equal to 60°C, T_{wo} takes a value thereabouts 78°C, which is equivalent to a gain of heating of 23 %. Therefore, according to these results, one can jump to the conclusion that it is interesting to work with low water temperature at the inlet of the water solar collector to allow the latter to provide a better gain of heating. Fig. 4 shows also the same result; for the low values of T_{ai}, T_{ao} can have high ones. So, as a conclusion, to obtain a better gain of heating both in water solar collector and air one, it is necessary to work with low values of inlet fluid temperatures.

Fig. 5 illustrates the impact of packed bed height on the outlet air humidity at the humidifier for different values of inlet air humidity. It transpires from Fig. 5 that the air humidity at the outlet of the humidifier varies linearly as a function of the packed bed height. This result is expected because the fact of augmenting the packed bed height will increase the contact area between air and water and, thus, increases the rate of air humidification. On the other hand, the air humidity at the inlet of the humidifier is the output of the condensation tower. So, its value is variable. Therefore it is interesting to perceive the influence of this parameter on air humidity at the outlet of the humidifier. From figure 5, one can also note that for the low values of W_{g1}, W_{g2} can have high ones. For example, for a 0.7

Table 2
Heat transfer correlations between water and inside vertical tube surface (h_e) [19]

Regime	Range	Heat transfer coefficient
Laminar	$Re < 2300$	$h_e = 3.66\frac{\lambda_e}{d_i}$
Transient	$2300 < Re < 10^4$	$h_e = \frac{\lambda_e}{d_i}\ 0.116\ (Re^{2/3} - 125)\ Pr^{1/3}\left(\frac{\mu}{\mu_p}\right)^{0.14}\left[1 + \left(\frac{d_i}{L}\right)^{2/3}\right]$
Turbulent	$Re > 10^4$	$h_e = \frac{\lambda_e}{d_i}\ 0.023\ Re^{0.8}\ Pr^{0.4}$

Table 3
Properties of the entire desalination unit used in simulation

Components	Description	Value/Type
Air solar collector	Aperture area	16 m^2
	Absorber plate material	Copper
	Absorptivity of plate	0.9
	Absorptivity of glass cover	0.1
	Back insulation, thickness	Polyurethane, 20 mm
	Emissivity of plate	0.94
	Emissivity of glass cover	0.987
	Transmissivity of glass cover	0.875
Water solar collector	Aperture area	7.2 m^2
	Effective transmission absorption	0.7
	Riser tubes materiel	Copper
	Absorber surface	Paint mat black
	Loss coefficient	4.8 $W/m^2.K$
	Back insulation, thickness	Fibre glass, 50 mm
Humidifier	Size	$0.5 \times 0.5 \times 0.7 m^3$
	Packed bed	Cellulosic materiel
	Mass transfer coefficient	$K_m = \left(0.6119\, m_L^{0.1002}\, m_g^{0.3753} Z^{-0.0986}\right) \Big/ a_h$
	Heat transfer coefficient	$h_L = \left(25223\, m_L^{0.0591}\, m_g^{0.1644} Z^{-0.0542}\right) \Big/ a_h$
	Air-film heat transfer coefficient	$h_g = C_g K_m$
Evaporation tower	Size	$0.5 \times 0.5 \times 1.5\ m^3$
	Packed bed	Thorn tree
	Mass transfer coefficient	$K_m = \left(2.09\, m_{L,ev}^{0.45}\, m_{g,ev}^{0.11515}\right) \Big/ a_{ev}$
	Heat transfer coefficient	$h_L = \left(5900\, m_{L,ev}^{0.169}\, m_{g,ev}^{0.5894}\right) \Big/ a_{ev}$
	Air-film heat transfer coefficient	$h_g = C_{g,ev} K_m$
	Heat transfer coefficient	$h_L = \left(5900\, m_{L,ev}^{0.169}\, m_{g,ev}^{0.5894}\right) \Big/ a_{ev}$
Condensation tower	Size	$0.5 \times 0.5 \times 1.5 m^3$
	Tubes type	Cuivre
	Inner diameter, d_i	0.014 m
	Outer diameter, d_e	0.012 m
	Tube length, L	1.5m
	Transverse pitch, P_t	0.050 m
	Longitudinal pitch, P_l	0.050 m

m of packed bed height and a value of W_{g1} equal to 0.02 kg water/kg dry air, W_{g2} takes a value of the order of 0.075 kg water/kg dry air, that is to say one can have a gain of humidification equal to 73.3%, while for a value of W_{g1} equal to 0.06 kg water/kg dry air, W_{g2} takes a value thereabouts 0.098 kg water/kg dry air, which is equivalent to a gain of humidification of 38.7%. Therefore, according to these results, one can infer the interest of working with low air humidity at the inlet of the humidifier to allow the latter to provide a better gain of humidification.

Fig. 6 presents the influence of the tube length on the fresh water production for various values of moist air flow rates. The first item that can be seen from this figure is that the fresh water production, m_c, increases with the moist air flow rate, m_{gt}. The obtained result can be explained by the fact that increasing the moist air flow rate is followed by mass and heat transfer coefficients increase inside the condensation tower, which ultimately raises the fresh water production water. The second item is that the fresh water production decreased with increased tube length but, after tube length of about 2 m, the rate of fresh water production drop was lower. This result may be due to the fact that the film condensation heat transfer coefficient for a vertical tube is inversely proportional to the tube length. So, increasing tube length (L) decreases the film condensation heat transfer coefficient which in its part

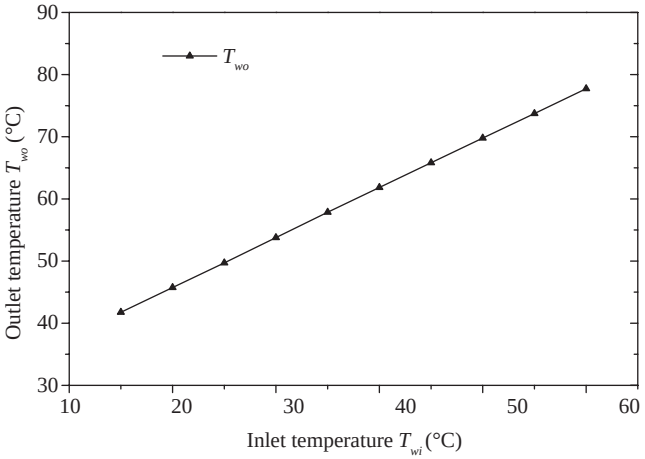

Fig. 3. Influence of the inlet water temperature on the outlet one at the water solar collector m_w=0.1 kg/s, T_{amb}=15°C, I=900 W/m^2.

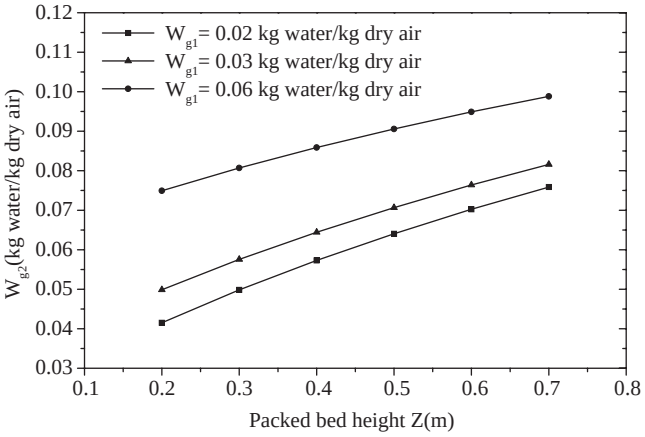

Fig. 5. Impact of the humidifier packed bed height on the outlet air humidity for different values of inlet one m_L=0.1 kg/s, m_g=0.2 kg/s, T_{l2}=60°C, T_{g1}=70°C.

decreases the quantity of condensed water. Furthermore, the condensation film is drained by the influence of the gravity alone in the downward direction of the condensation tower. Consequently, increasing the tube length will increase the thickness of the condensation film and, thus, creates an additional thermal resistance. This leads to decreasing the fresh water production.

In Figs. 7 and 8, we present respectively the influence of the inlet cooling water temperature at the bottom of the condensation tower and that of the inlet moist air temperature at the top of the condensation tower on the fresh water production. According to these figures, it is clear that the moist air and cooling inlet temperatures have an antagonist impact on the fresh water production. In fact, the amount of condensed water decreases significantly when T_{e1} increases and it increases significantly when T_{gc2} increases

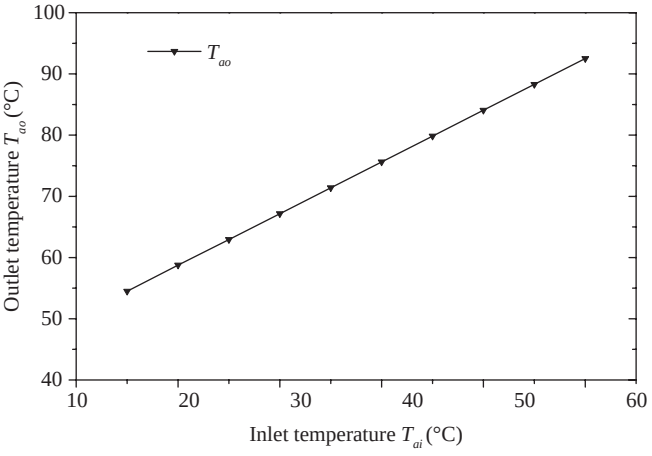

Fig. 4. Influence of the inlet air temperature on the outlet one at the air solar collector m_a=0.1 kg/s, T_{amb}=15°C, I=900 W/m^2.

Fig. 9 shows the effect of inlet water temperature at the evaporation tower on fresh water production (m_c), it is clear that the fresh water production increases linearly with inlet water temperature at the evaporation tower. It also shows a comparison between present unit and Ben Bacha's without taking account of the design's properties of each component constituting the compared units. With reference to Fig. 9, it is clear that the production of fresh water of the present unit (water solar collector, air solar collector, evaporation tower, humidifier and condensation tower) is increased by 65.7% for low values of water temperatures thereabouts 45°C and by 34.18% for the high values of water temperatures thereabouts 70°C by comparison to Ben Bacha's unit [3] (water solar collector, evaporation tower and condensation tower).

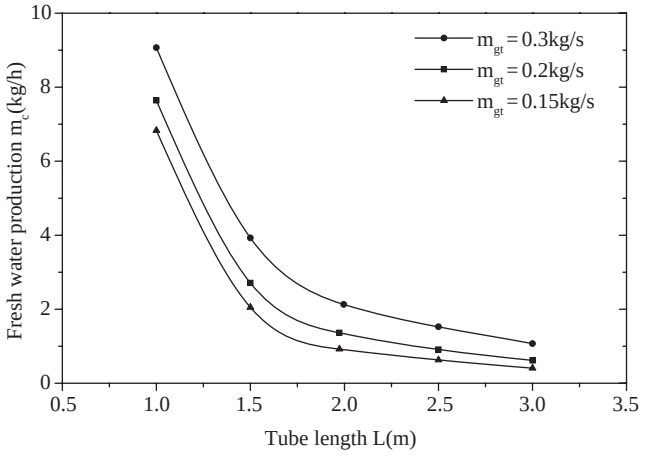

Fig. 6. Influence of the condensation tower tube length on the fresh water production for various values of air flow rates D_e=0.1 kg/s, T_{gc2}=70°C, W_{gc2}=0.287 kg water/kg dry air.

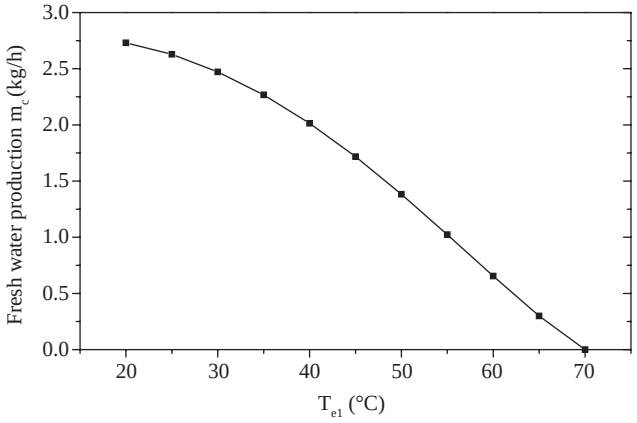

Fig. 7. Influence of the inlet cooling water temperature on the fresh water production *De*= 0.1 kg/s, m_{gt}=0.2 kg/s, T_{gc2}=70°C, W_{gc2}= 0.287 kg water/kg dry air.

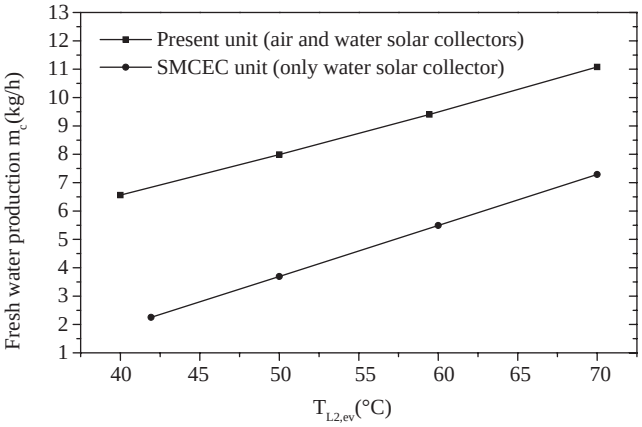

Fig. 9. Effect of inlet water temperature at the evaporation tower on fresh water production (comparison between present unit and the SMCEC unit developed by Ben Bacha el al. [3]).

5. Conclusion

This paper presents a theoretical study of a new design process working with humidification dehumidification (HD) technique using solar energy which is developed in order to ameliorate the production of the SMCEC unit (Solar Multiple Condensation Evaporation Cycle). So the unit is made up of five components: air solar collector, water solar collector, humidifier, evaporation tower and condensation tower. A global mathematical model expressing the heat and mass transfers in each component of the unit is formulated. The developed model is simulated, using the Borland C++ software to study the behavior of key output parameters for each component of the unit. According to the simulation results, it is interesting to work with:

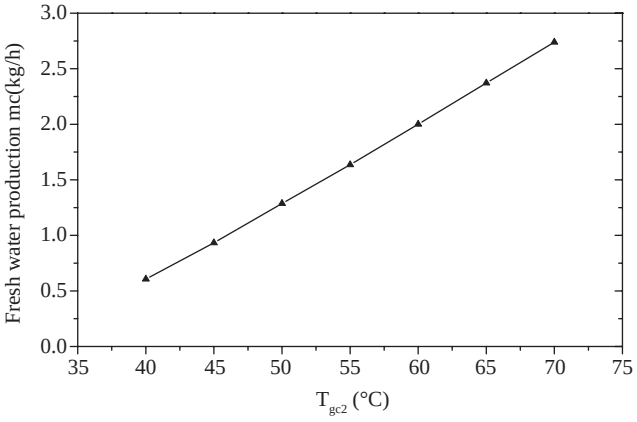

Fig. 8. Influence of the inlet moist air temperature on the fresh water production *De*= 0.1 kg/s, m_{gt}=0.2 kg/s, T_{e1}=20°C, W_{gc2}= 0.287 kg water/kg dry air.

- Low values of inlet fluid temperatures at the level of both air and water solar collectors in order to obtain a better gain of heating.
- Low air humidity at the inlet of the humidifier to allow the latter to provide a better gain of humidification.
- High values of moist air flow rate at the level of the condensation tower to provide a better fresh water production.
- High values of inlet moist air temperature at the top of the condensation tower
- High values of inlet water temperature at the evaporation tower
- Low values of inlet cooling water temperature at the bottom of the condensation tower

Acknowledgements

The authors wish to express their deepest thanks and heartfelt appreciation to the Ministère de l'Enseignement Supérieur et de la Recherche Scientifique and to the Agence Nationale de la Maîtrise de l'Energie (ANME) for their financial support.

It goes without saying that special thanks should be darted at the English teacher Mr. R.Romdhani

Symbols

A	air-water exchanger area in the condensation tower (m^2)
a	air-water exchanger area (m^2)
b	width of air solar collector (m)
B	effective transmission absorption product ($B = \tau\alpha$)
C_e	water specific heat (J/(kg K))
C_w	water specific heat (J/(kg K))

C_g moist air specific heat in the humidifier (J/(kg K))
C_{gc} moist air specific heat in the condensation tower (J/(kg K))
$C_{g,ev}$ moist air specific heat in the evaporation tower (J/(kg K))
D_e water mass velocity in the condensation tower (kg/(m^2 s))
d_e outer diameter of the condensation tower tube (m)
d_i inner diameter of the condensation tower tube (m)
g gravitational acceleration (m/s^2)
h heat transfer coefficient (J/(kg K))
h_g air heat transfer coefficient at the air-water interface(W/(m^2 K))
h_e water heat transfer coefficient at the air-water interface(W/(m^2 K))
l width of water solar collector (m)
L tube length of the condensation tower (m)
I solar flux (W/m^2)
K_m water vapor mass transfer coefficient at the air-water interface (kg/(m^2 s))
m mass flow rate (kg/s)
m_c fresh water production (kg/s)
m_{gt} total mass velocity of moist air in the condenser (kg/(m^2 s))
Pr Prandtl number
Re Reynolds number
P_i saturation pressure (Pa)
P_l longitudinal pitch (m)
P_t transverse pitch (m)
T temperature (K)
T_i temperature at the air-water interface (K)
U overall heat transfer coefficient in the condensation tower (W/ (m^2 K))
U_w overall energy loss from the absorber to outside (W/ (m^2 K))
W air humidity (kg water/kg dry air)
W_i saturation humidity (kg water/kg dry air)
Z height of the humidifier packed bed (m)
z coordinate in the flow direction (m)
x coordinate in the flow direction (m)

Greek

α absorptance of the collector absorber surface
λ_o latent heat of water evaporation (J/kg)
λ_p wall thermal conductivity (W/m K)
λ_e water thermal conductivity (W/m K)
λ_c condensed water thermal conductivity (W/m K)
λ_{gc} humid air thermal conductivity in the condensation tower (W/m K)
ρ_c water density (kg/m^3)
μ_c dynamic viscosity of condensed water (Ns/m^2)
μ_p dynamic viscosity at the wall temperature (Ns/m^2)
σ Stefan-Boltzman constant
υ velocity of fluid (m/s)
τ transmittance

Subscripts

1 tower bottom
2 tower top
a air
amb ambient
c condensation tower
con convection
e cooling water
v glass cover
ev evaporation tower
w water
g moist air
h humidifier
loss loss to ambient
pl absorber plate
rad radiation

References

[1] A. Soteris, Seawater desalination using renewable energy sources. Progr. Energy Combust. Sci., 31 (2005) 242–281.
[2] H. Ben Bacha, M. Bouzguenda, M.S. Abid and A.Y. Maalej, Modeling and simulation of a water desalination station with solar multiple condensation evaporation cycle technique, Renewable Energy, 18 (1999) 349–365.
[3] S.M. Soufari, M. Zamen and M. Amidpour, Experimental validation of an optimized solar humidification-dehumidification desalination unit, Desalination Water Treat., 13 (2010) 96–108.
[4] M. Ben Amara, I. Houcine, A.A. Guizani and M. Maalej, Experimental study of a multiple-effect humidification solar desalination technique, Desalination, 170 (2004) 209–221.
[5] M. Ben Amara, I. Houcine, A.A. Guizani and M. Maalej, Comparison of indoor and outdoor experiments on a newly designed air solar plate collector used with the operating conditions of a solar desalination process, Desalination, 168 (2004) 81–88.
[6] J. Orfi, N. Galanis and L. Laplante, Air humidification–dehumidification for a water desalination system using solar energy, Desalination, 203 (2007) 471–481.
[7] K. Bourouni, R. Martin, L. Tadrist and H. Tadrist, Experimental investigation of evaporation performances of a desalination prototype using the aeroevapo-condensation process, Desalination, 114 (1997) 111–128.
[8] N.K. Nawayseh, M.M. Farid, A.A. Omar, S.M. Al- Hallaj and A.R. Tamimi, A simulation study to improve the performance of a solar humidification– dehumidification desalination unit constructed in Jordan, Desalination, 109 (1997) 277–284.
[9] S. Al-Hallaj, M.M. Farid and A.R. Tamimi, Solar desalination with a humidification–dehumidification cycle: performance of the unit, Desalination, 120 (1998) 273–280.

[10] Y.J. Dai and H.F. Zhang, Experimental investigation of a solar desalination unit with humidification– dehumidification, Desalination, 130 (2000) 169–175.
[11] S.A. Hashemifard and R. Azin, New experimental aspects of the carrier gas process (CGP), Desalination, 164 (2004) 125–133.
[12] S. Parekh, M.M, Farid, J.R. Selman and S. Al-Hallaj, Solar desalination with a humidification dehumidification technique a comprehensive technical review, Desalination, 160 (2004) 167–186.
[13] K. Zhani, H. Ben Bacha and T. Damak. A study of a water desalination unit using solar energy, Desalination Water Treat. 3 (2009) 261–270.
[14] K. Zhani and H. Ben Bacha, An approach to optimize the production of solar desalination unit using the SMCEC principle, Desalination Water Treat., 13 (2010) 96–108.
[15] ASHRAE, Fundamental handbook TomeV- 1977.
[16] F. Incropera, D. dewitt, T. Bergman and A. Lavine, Fundamental of heat and mass transfer, 6th ed. Wiley, 2007.
[17] H.T. El-Dessouky, H.M. Ettouney and Y.Al-Roumi, Multi-stage Flash desalination: present and future outlook, Chem. Eng. J., 73 (1999) 173–190.
[18] P. Panday, Transferts en changement de phase. Condensation sur des surfaces lisses, BE 8239, Traité Génie énergétique, Techniques de l'Ingénieur (2006).
[19] Adrian Bejan and Allan D. Kraus, Heat transfer handbook, first ed. John Wiley & Sons, INC., Hoboken, New Jersey, 2003.
[20] Robert H. Perry, Donald W. Green and Don Green, Perry's Chemical Engineers' Handbook, seventh ed. McGraw-Hill Professional, 1997.